
Spatiotemporal Variation and Influencing Factors of Ecological Quality in the Guangdong-Hong Kong-Macao Greater Bay Area Based on URSEI over the Past 30 Years

[Fangfang Sun](#) , [Chengcheng Dong](#) , [Longlong Zhao](#) , [Jinsong Chen](#) , Li Wang , [Ruixia Jiang](#) * , [Hongzhong Li](#) *

Posted Date: 14 April 2025

doi: 10.20944/preprints202504.1092.v1

Keywords: Ecological quality; URSEI; Spatial autocorrelation; Influencing factors; Geographical Detector; Guangdong-Hong Kong-Macao Greater Bay Area (GBA)



Preprints.org is a free multidisciplinary platform providing preprint service that is dedicated to making early versions of research outputs permanently available and citable. Preprints posted at Preprints.org appear in Web of Science, Crossref, Google Scholar, Scilit, Europe PMC.

Copyright: This open access article is published under a Creative Commons CC BY 4.0 license, which permit the free download, distribution, and reuse, provided that the author and preprint are cited in any reuse.

Article

Spatiotemporal Variation and Influencing Factors of Ecological Quality in the Guangdong-Hong Kong-Macao Greater Bay Area Based on URSEI over the Past 30 Years

Fangfang Sun ^{1,†}, Chengcheng Dong ^{1,†}, Longlong Zhao ², Jinsong Chen ², Li Wang ³, Ruixia Jiang ^{2,3,*} and Hongzhong Li ^{2,*}

¹ Shenzhen Academy of Environmental Science, Shenzhen 518001, China

² Shenzhen Institutes of Advanced Technology, Chinese Academy of Sciences, Shenzhen 518055, China

³ School of Surveying and Land Information Engineering, Henan Polytechnic University, Jiaozuo 454003, China

* Correspondence: rx.jiang1@siat.ac.cn (R.J.); hz.li@siat.ac.cn (H.L.); Tel.: +86-156-7088-5517 (R.J.); Tel.: +86-137-2349-2858 (H.L.)

† Co-first author, these authors contributed equally to this work.

Abstract: The Guangdong-Hong Kong-Macao Greater Bay Area (GBA) is one of China's three major urban agglomerations. Over the past thirty years, the region has undergone intensive economic development and urban expansion, resulting in significant changes in its ecological conditions. Due to the region's humid and rainy climate, traditional remote sensing ecological index (RSEI) struggle to ensure consistency in long-term ecological quality assessments. To address this, the study developed a Unified RSEI (URSEI) model, incorporating optimized data selection, composite index construction, normalization using invariant regions, and multi-temporal principal component analysis. Using Landsat imagery from 1990 to 2020, the study examined the spatiotemporal evolution of ecological quality in the GBA. Building on this, spatial autocorrelation analysis was applied to explore the distribution characteristics of URSEI, followed by Geodetector analysis to investigate its driving factors, including temperature, precipitation, elevation, slope, land use, population density, GDP, and nighttime light. The results indicate that: (1) URSEI effectively mitigates the impact of cloudy and rainy conditions on data consistency, producing seamless ecological quality maps that accurately reflect the region's ecological evolution; (2) Ecological quality showed a "decline-then-improvement" trend during the study period, with the URSEI mean dropping from 0.65 in 1990 to 0.60 in 2000, then rising to 0.63 by 2020. Spatially, ecological quality was higher in the northwest and northeast, and poorer in the central urbanized areas; (3) In terms of driving mechanisms, nighttime light, GDP, and temperature were the most influential, with the combined effect of "nighttime light + land use" being the primary driver of URSEI spatial heterogeneity. Human activity-related factors showed the most notable variation in influence over time.

Keywords: ecological quality; URSEI; spatial autocorrelation; influencing factors; geographical detector; Guangdong-Hong Kong-Macao Greater Bay Area (GBA)

1. Introduction

The ecological environment is the foundation of human survival and social development, and its condition and evolution are directly linked to human existence and sustainable development. Over the past half-century, rapid population growth and advancements in science and technology have accelerated the exploitation of natural resources in both scale and intensity. While these activities have brought substantial material wealth to human society, they have also exacerbated

ecological imbalances. Issues such as vegetation destruction, climate change, water shortages, land degradation, and biodiversity loss have become increasingly prevalent, posing significant threats to regional ecological security and economic sustainability [1–3]. Accurately understanding and assessing regional ecological conditions, clarifying their changing trends, and identifying driving mechanisms are fundamental to environmental protection. These efforts also serve as a critical basis for formulating environmental policies and resource development plans [4–6].

In recent years, remote sensing technology has become an essential tool for regional ecological quality assessment due to its advantages of fast processing speed, wide coverage, and high timeliness. Many scholars have used remote sensing indices to evaluate ecological conditions, such as monitoring changes in vegetation cover through vegetation indices [7–9], studying urban heat island effects using surface temperature data [10,11], and assessing regional water environments through water indices to extract river information [12]. However, ecological conditions are a complex system influenced by multiple factors, and independent evaluations based on a single indicator can only reflect a specific aspect of the ecosystem, making it difficult to fully and accurately capture the overall ecological quality [13–16]. In response, Professor Xu Hanqiu [17] proposed the Remote Sensing Ecological Index (RSEI) in 2013. This index, entirely based on remote sensing technology, integrates four indicators: greenness, humidity, heat, and dryness, enabling a comprehensive assessment of ecological conditions. It also visually reflects spatial variations in regional ecological quality, and has been widely applied in different regions [18–20]. As the application of RSEI in ecological monitoring has expanded, many scholars have improved the method by refining aspects such as indicator selection [21,22], normalization [23], and indicator synthesis [24,25] to meet the ecological assessment needs of various regions. These improvements have enhanced the applicability of RSEI in regional ecological monitoring, yielding positive results. Therefore, to more accurately monitor and assess regional ecological quality, developing a more refined regional remote sensing ecological index is essential [26].

The changes in ecological quality are influenced by multiple factors. In addition to natural factors, human activities are considered to be a major driving force behind the decline in ecological quality in some cases [27–30]. However, most studies focus primarily on analyzing the ecological quality of a study area and its spatiotemporal changes, with limited exploration of the specific factors driving these changes [31,32]. In fact, a thorough analysis of driving factors can more precisely reveal the root causes of ecological issues, providing a scientific basis for ecological protection and sustainable development [33]. Common methods for analyzing influencing factors include correlation coefficient methods [34,35], elasticity coefficient methods [36], panel quantile regression [37], and geographically weighted regression [38]. While these methods can effectively assess the impact of multiple factors, they struggle to uncover the interactions between factors and their combined effects on ecological quality changes. To address this limitation, Wang Jinfeng et al. [39] proposed the Geographical Detector Model, a statistical method for detecting spatial heterogeneity and revealing underlying driving factors. This model not only quantitatively analyzes the explanatory power of each driving factor on ecological changes but also detects the interaction effects of driving factors on ecological quality. It has been widely applied in fields such as land use [40], regional economy [41], meteorology [42], environment [43], and public health [44].

The Guangdong-Hong Kong-Macao Greater Bay Area (GBA) is the fourth largest bay area in the world, following the New York Bay Area, San Francisco Bay Area, and Tokyo Bay Area. It serves as an important spatial platform for the country's development of a world-class city cluster and participation in global competition. Over the past few decades, the rapid economic development and urban expansion in the GBA have disrupted the original ecological system elements, structure, and functions, presenting severe challenges to ecological civilization construction. Timely and accurate acquisition of the spatiotemporal distribution characteristics, evolution trends, and driving mechanisms of ecological quality in the GBA is of great significance for promoting ecological governance and protection of urban environments. Given that the GBA is located in South China, with a consistently cloudy and rainy climate, and experiences dramatic ecological changes, the use

of RSEI for long-term ecological monitoring and assessment is often affected by cloud cover in optical imagery. This impact influences various aspects, such as regional image stitching, indicator extraction, normalization, and consistency of data acquisition across different time phases, ultimately affecting the spatiotemporal comparability of ecological indices and the accuracy of evolution pattern analysis. In previous studies on long-term ecological quality assessment in the GBA, the comparability of time series has been relatively low, making it difficult to accurately reflect the spatiotemporal distribution and evolution patterns of ecological quality [45–48].

To address this issue, based on the RSEI, a Unified Remote Sensing Ecological Index (URSEI) was developed by optimizing indicator selection, normalizing invariant regional indicators, and integrating multi-temporal principal component analysis. This method is designed for long time series and regions with dramatic ecological changes. Using long-term satellite remote sensing data, the study analyzed the spatiotemporal distribution patterns and evolution trends of ecological environmental quality in the GBA from 1990 to 2020. Spatial autocorrelation analysis was then applied to investigate the spatial clustering of ecological indices in the GBA. Furthermore, the Geographical Detector Model was employed to quantitatively explore the impact mechanisms of natural factors such as topography and climate, and human factors such as land use types and population density, on the spatial differentiation of ecological quality. The findings contribute to a comprehensive understanding of the ecological environment in the GBA and its driving mechanisms, providing a scientific basis for regional ecological protection and governance.

2. Materials and Methods

2.1. Study Area

The GBA is located in the central and southern part of Guangdong Province (21°32'–24°26'N, 111°20'–115°24'E), covering an area of approximately 56,000 km². It includes nine cities in Guangdong Province: Guangzhou, Shenzhen, Zhuhai, Foshan, Dongguan, Zhongshan, Jiangmen, Huizhou, and Zhaoqing, as well as the two Special Administrative Regions of Hong Kong and Macao. The region has a unique topography, surrounded by hilly and mountainous terrain in the west, north, and east, with a vast plain in the center. The southern part faces the South China Sea, forming a geographical pattern of "mountains on three sides, the sea on one side," with the terrain gradually descending from the northwest and northeast toward the central and southern parts. The GBA has a subtropical humid monsoon climate with abundant rainfall, receiving an annual precipitation of 1900–2000 mm and a mild climate, with an average annual temperature of 21–23°C. Thanks to its favorable geographical conditions and strong national policy support, the region has experienced rapid economic development and has become one of the fastest urbanizing, most open, and economically dynamic regions in China. As of 2024, the GBA's permanent population has reached 86.17 million, with a population density of 1531 people per km².

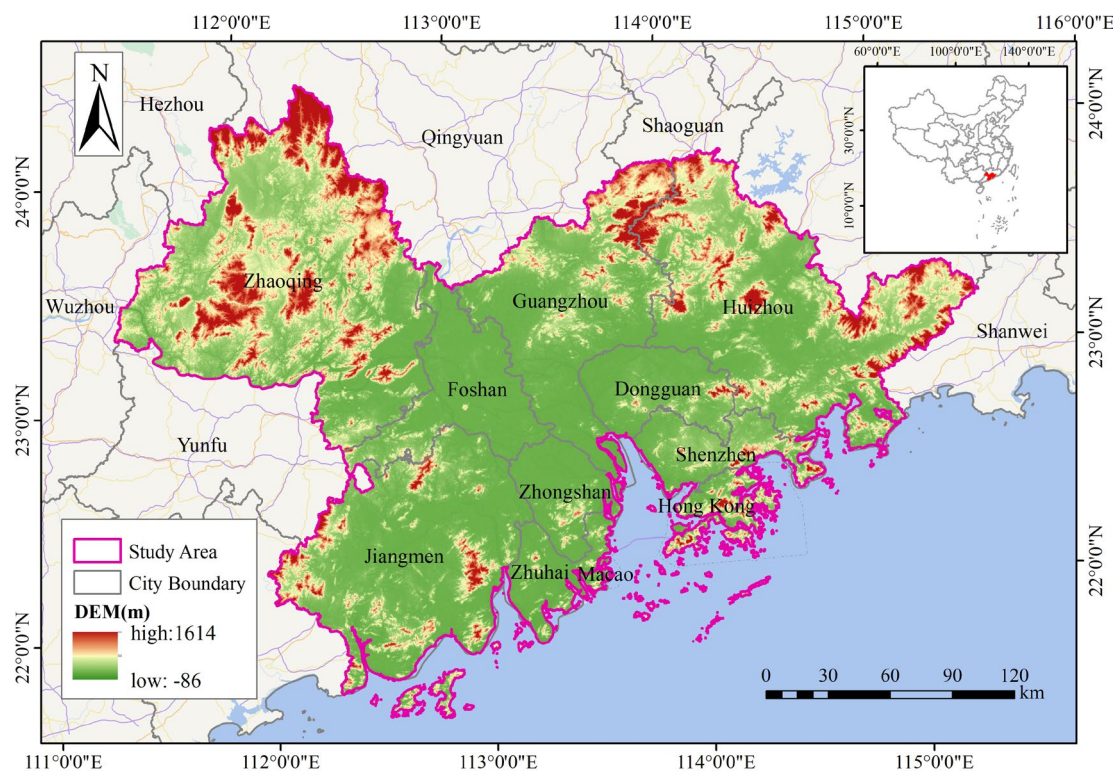


Figure 1. Location of the GBA, China.

2.2. Data Sources and Preprocessing

2.2.1. Remote Sensing Data and Preprocessing

The study utilizes Landsat series remote sensing images provided by NASA (<https://images.nasa.gov/>) as the primary data source. Landsat-5 TM images were selected for the years 1990, 2000, and 2010, while Landsat-8 OLI images were used for 2020. Given the long acquisition cycle of Landsat data and the frequent cloud cover in the GBA, images were selected from the target year and the adjacent years within the vegetation growth period (September, October) and the non-growth period (December, January), ensuring cloud coverage below 30%. Data preprocessing included cloud removal and water masking. Cloud removal was performed using the CFMASK algorithm based on the QA quality assessment band of Landsat images. Additionally, permanent water bodies, including rivers and reservoirs, were masked using the secondary wetland category from the 1990–2020 land cover product of the Greater Bay Area [49] to minimize the impact of surface water on the humidity principal component load.

2.2.2. Impact Factor Data and Preprocessing

The driving factors influencing the distribution and evolution of ecological quality can be categorized into natural and anthropogenic factors. Based on previous studies [50–53] and data availability, this study selects four natural factors—temperature, precipitation, elevation, and slope—and four anthropogenic factors—land use type, population density, GDP, and nighttime light index. The primary data sources and details are listed in Table 1. Since nighttime light and GDP data for 1990 are unavailable, the study substitutes them with data for 1992.

The preprocessing of driving factor data was conducted primarily using ArcGIS 10.2. Due to inconsistencies in spatial extent and projection among different datasets, all data were first clipped and reprojected to align with the study area. Additionally, considering variations in spatial resolution, all datasets were resampled to a uniform resolution of 1 km × 1 km.

Since the geographical detector model used in the subsequent analysis requires categorical variables, the independent variables were reclassified. Land use type data were classified into six

categories based on product specifications, while other numerical driving factors were discretized into five categories using the natural breaks method in ArcGIS.

Table 1. Main information and sources of impact factor data.

Data	Time	Resolution	Data source
Temperature	1990, 2000, 2010, 2020	1km	http://www.geodata.cn/
Precipitation	1990, 2000, 2010, 2020	1km	
Population density	1990, 2000, 2010, 2020	1km	https://www.resdc.cn/
Nighttime lights	1990, 2000, 2010, 2020	1km	https://dataverse.harvard.edu/
GDP	1990, 2000, 2010, 2020	1km	https://www.resdc.cn/
Type of land use	1990, 2000, 2010, 2020	30m	ChinaCover
DEM	--	30m	https://www.gscloud.cn/

2.3. Construction of the URSEI

2.3.1. Indicator Factors

The Remote Sensing Ecological Index (RSEI) model integrates four key indicator factors closely related to human daily life: greenness, humidity, heat, and dryness. Specifically, the Normalized Difference Vegetation Index (NDVI) represents the greenness indicator, the humidity component (WET) derived from tasseled cap transformation represents surface moisture, the average synthesis of the Index-Based Built-up Index (IBI) and the Soil Index (SI) serves as the dryness indicator (NDBSI), and the Land Surface Temperature (LST) represents the heat indicator. These four indicators are entirely derived from remote sensing data, making them easily accessible, with a computational process that requires no manual intervention, ensuring objective and reliable results. The Unified Remote Sensing Ecological Index (URSEI) retains the four indicator factors of RSEI, with the calculation methods for each ecological indicator shown in Table 2.

Table 2. The calculation method of ecological indicators.

Index	Calculation Methods
NDVI	$NDVI = (B_{nir} - B_{red}) / (B_{nir} + B_{red}) \quad (1)$
	$SI = \frac{[(B_{swir1} + B_{red}) - (B_{nir} + B_{blue})]}{[(B_{swir1} + B_{red}) + (B_{nir} + B_{blue})]} \quad (2)$
NDBSI	$IBI = \frac{2B_{swir1} / (B_{swir1} + B_{nir}) - [B_{nir} / (B_{nir} + B_{red}) + B_{green} / (B_{green} + B_{swir1})]}{2B_{swir1} / (B_{swir1} + B_{nir}) + [B_{nir} / (B_{nir} + B_{red}) + B_{green} / (B_{green} + B_{swir1})]} \quad (3)$
	$NDBSI = (SI + IBI) / 2 \quad (4)$
	$TM : WET = 0.0315 \times B_{blue} + 0.2021 \times B_{green} + 0.3012 \times B_{red} + 0.1594 \times B_{nir} - 0.6806 \times B_{swir1} - 0.6109 \times B_{swir2} \quad (5)$
WET	$OLI : WET = 0.1511 \times B_{blue} + 0.1973 \times B_{green} + 0.3283 \times B_{red} + 0.3407 \times B_{nir} - 0.7117 \times B_{swir1} - 0.4559 \times B_{swir2} \quad (6)$
LST	The study selects the land surface temperature (LST) from the Landsat SR product as the LST indicator factor. (7)

Note: B_{red} , B_{blue} , B_{green} , B_{nir} , B_{swir1} , and B_{swir2} represent the reflectance of the Landsat imagery in the red, blue, green, near-infrared (NIR), shortwave infrared 1 (SWIR1), and shortwave infrared 2 (SWIR2) bands, respectively.

2.3.2. Synthesis of Indicator Factors

In this study, multiple images were selected for each monitoring year, necessitating a synthesis process to generate the four indicator factors for each monitoring period. For greenness, humidity, and dryness indicators, a median composite was first applied separately to the vegetation growing season and the non-growing season images, followed by averaging the results from both periods. The median composite effectively reduces the influence of weather conditions, precipitation, and solar altitude angle, minimizing anomalies and ensuring that the indicators accurately reflect the average conditions of each period. This approach prevents extreme observations from skewing the overall assessment. The final averaging process provides a more comprehensive representation of the ecological conditions throughout the year, mitigating potential biases from single-period observations and delivering a more stable and integrated ecological evaluation.

$$I_y = \frac{1}{2}(I_y^a + I_y^w) \quad (8)$$

$$I_y^a = \text{Median}\{I_{y_i}^{d_j}\} \quad (9)$$

$$y - 1 \leq y_i \leq y + 1 \quad d_j \in \{a\}$$

$$I_y^w = \text{Median}\{I_{y_i}^{d_j}\} \quad (10)$$

$$y - 1 \leq y_i \leq y + 1 \quad d_j \in \{w\}$$

where I represents the indicator factor, y denotes the year, a represents the vegetation growing season, w represents the non-growing season, and Median denotes the median operator, $I_{y_i}^{d_j}$ represents the I indicator on date d_j of year y_i .

For the heat indicator, imagery from the autumn vegetation growing season is selected for each monitoring period. The Landsat thermal infrared data from path/row 122/44 at the center of the study area is used as the reference. A random forest regression model is applied to calibrate the thermal infrared data from other path/row numbers using overlapping areas, generating temperature-consistent thermal infrared data aligned with the reference (122/44). A median operator is then used to synthesize the thermal infrared data for the entire GBA. In the random forest regression model, input variables include land cover type, elevation, slope, NDVI, NDWI, WET, IBI, and SI.

2.3.3. Indicator Normalization Based on Invariant Regions

The RSEI model employs range normalization to eliminate dimensional differences among indicators. However, this method is susceptible to extreme values, which may introduce biases in the results. Over the past 30 years, the Greater Bay Area has undergone significant urban expansion and ecological changes, leading to substantial differences in the statistical distribution of ecological indicators. While conventional probability-based normalization methods (such as Z-score or Gaussian normalization) can adjust data distribution, they may reduce time-series consistency, affecting the spatial-temporal comparability of indicators and the accuracy of evolution pattern analysis.

To address the issue of indicator normalization, this study proposes an invariant-region-based normalization method. First, a 30-year invariant region layer is constructed based on the land cover data of the Greater Bay Area from 1990 to 2020. By comparing land cover changes across different years, regions with no significant changes are identified using the following formula:

$$U = U_1 \cap U_2 \cap U_3 \quad (11)$$

U_1 , U_2 , and U_3 represent the land cover layers for the periods 1990-2000, 2000-2010, and 2010-2020, where no changes in land cover occurred; U represents the intersection of the three invariant region layers.

Then, based on the invariant layer U , the indicator factors for different monitoring periods are masked. The cumulative probability distribution function method is applied to calculate the 1st and 99th percentiles of the masked indicators, which are used as the minimum and maximum values. Finally, these statistical results are used to normalize the original, non-masked indicator factors, ensuring that their range is constrained between 0 and 1. At the same time, dryness and heat are treated as negative indicators and undergo reverse normalization to ensure that the negative indicators are reasonably reflected in the overall ecological assessment.

2.3.4. Multi-Temporal Fusion Principal Component Analysis

The RSEI model uses Principal Component Analysis (PCA) to construct a composite ecological index for each monitoring period and standardizes the RSEI values to a range of 0-1 using range normalization, effectively reflecting the relative ecological condition of a specific spatial region at a given time. However, in areas with significant ecological changes, the RSEI value only represents the relative condition within a specific period, making it difficult to accurately reflect the long-term ecological evolution trend across different years.

In this study, ecological indicator factors from four monitoring periods are fused using a unified principal component analysis to construct a composite ecological index. First, the normalized indicator factors are used as variables, and they are input into PCA synchronously and with equal weight to ensure that the data are processed under the same standard. Then, the contribution rate of the first principal component (PC1) is assessed. If it exceeds 70%, PC1 can be used to create the composite ecological index. Unlike the traditional RSEI model, this study does not re-normalize the composite ecological index. Instead, it normalizes the feature vector of PC1 and applies it uniformly to all monitoring periods to generate the Unified Remote Sensing Ecological Index (URSEI), ensuring the comparability of ecological quality changes across different time periods. The formula is as follows:

$$[\lambda_1, \lambda_2, \lambda_3, \lambda_4] = \text{PC1}(\text{NDVI}, \text{WET}, \text{NDBSI}, \text{LST}) \quad (12)$$

$$\text{URSEI} = \lambda_1 \text{NDVI} + \lambda_2 \text{WET} + \lambda_3 \text{NDBSI} + \lambda_4 \text{LST} \quad (13)$$

where, λ_i is the eigenvector of PC1, satisfying $\sum \lambda_i^2 = 1$.

2.4. Average Correlation

Average correlation \bar{C} is used in this study to test the applicability of URSEI. A value close to 1 indicates a higher degree of comprehensive representation by the model, signifying stronger applicability. The formula is as follows:

$$\bar{C} = \frac{(|C_p| + |C_q| + |C_r| + |C_g|)}{n}$$

where C_p , C_q , C_r and C_g represent the correlation coefficients of the p , q , r , and g indicators at the same time, and n is the number of indicators.

2.5. Spatial Autocorrelation Analysis

Spatial autocorrelation analysis is used to test whether the attribute values of elements with spatial locations are related to the attribute values at neighboring spatial points. It is an important indicator of the aggregation or dispersion of spatial elements. It includes both global spatial autocorrelation and local spatial autocorrelation [54–57]. By calculating the global Moran's I index, it can be used to analyze the overall spatial correlation and spatial differences in the region during different periods. The formula is as follows:

$$I_g = \frac{n \sum_{i=1}^n \sum_{j=1}^n (X_i - \bar{X})(X_j - \bar{X})}{(\sum_{i=1}^n \sum_{j=1}^n W_{ij}) \sum_{i=1}^n (X_i - \bar{X})^2}$$

where n is the number of samples, X_i and X_j are the attribute values of X at spatial locations i and j , \bar{X} is the average value of attribute X_i , and W_{ij} is the spatial weight matrix. The range of Moran's I index is $(-1, 1)$. When $I_g > 0$, it indicates a positive correlation between spatial units; when $I_g < 0$, it indicates a negative correlation between spatial units; when $I_g = 0$, it indicates no correlation, representing a random distribution.

The local Moran's I index can be used to assess the correlation and significance between a region and neighboring regions, and to visualize it using the Local Indicators of Spatial Association (LISA). The calculation formula for the local Moran's I is as follows:

$$I_i = \frac{n(X_i - \bar{X}) \sum_{j=1}^n W_{ij}(X_j - \bar{X})}{\sum_{i=1}^n (X_i - \bar{X})^2} \quad (16)$$

where the meanings of the parameters are the same as in the previous formula (15).

2.6. Geographical Detector

The geographical detector is a statistical model proposed by Wang Jinfen et al., specifically designed to detect spatial differentiation characteristics and their driving mechanisms. In this study, the eight driving factors from Section 2.2.2 are used as independent variables X , with URSEI values as the dependent variable Y . The factor detector, interaction detector, and risk zone detector in the geographical detector are used to systematically explore the impact and interrelationships of various factors on the spatial differentiation of ecological quality.

(1) Factor Detection: This is used to analyze the extent to which the selected independent variables X explain the spatial differentiation of the dependent variable Y (URSEI) at different time stages. Its explanatory power is measured by the q -value, as:

$$q = 1 - \frac{\sum_{h=1}^L N_h \sigma_h^2}{N \sigma^2} \quad (17)$$

where L represents the stratification of the independent variable X , i.e., the number of categories; N_h and N are the number of sampling points in the h -th category of the independent variable X and the total number of sampling points in the region, respectively; σ_h^2 and σ^2 are the variances of the h -th category region for the independent variable X and the variance of Y across the entire region, respectively; the range of q is from 0 to 1. The larger the q value, the stronger the explanatory power of the independent variable X on the dependent variable Y , and vice versa. The q value indicates that X explains 100 $q\%$ of Y .

(2) Interaction detection: This is used to identify the interactions between different influencing factors X_i and assess how the explanatory power of the dependent variable Y changes when two factors (such as X_1 and X_2) act together. The interactions between factors can be divided into five types, and their corresponding q -value ranges are shown in Table 3.

Table 3. Interaction types of the detection factors.

Q-value range	The type of interaction
$q(X_1 \cap X_2) < \min[q(X_1), q(X_2)]$	Nonlinear weakening
$\min[q(X_1), q(X_2)] < q(X_1 \cap X_2) < \max[q(X_1), q(X_2)]$	Univariate nonlinear weakening
$q(X_1 \cap X_2) > \max[q(X_1), q(X_2)]$	Bivariate enhancement
$q(X_1 \cap X_2) = q(X_1) + q(X_2)$	Independence
$q(X_1 \cap X_2) > q(X_1) + q(X_2)$	Non-linear enhancement

(3) Risk zone detection: This is used to evaluate whether there is a significant difference in the mean of the dependent variable Y between any two sub-regions within the different strata of the independent variable X , and to conduct significance testing using the t -statistic."

$$t_{\bar{y}_{h=1}-\bar{y}_{h=2}} = \frac{\bar{Y}_{h=1} - \bar{Y}_{h=2}}{\left[\frac{Var(\bar{Y}_{h=1})}{n_{h=1}} + \frac{Var(\bar{Y}_{h=2})}{n_{h=2}} \right]^{1/2}} \quad (18)$$

where \bar{Y}_h is the mean URSEI value in region h , n_h is the sample size within the sub-region, and Var represents variance.

3. Results

3.1. Model Validation

Table 4 presents the principal component analysis results for the four monitoring periods from 1990 to 2020 and the fused data, including the eigenvalue and contribution rate of the first principal component (PC1), as well as the corresponding eigenvectors for each indicator factor in PC1. As shown in Table 4, the contribution rate of PC1 exceeds 75% for each period, and for the fused and unified principal component analysis result, the contribution rate of PC1 reaches 81.6%. This indicates that PC1 integrates the majority of the characteristics of the four indicator factors and can be used to create the comprehensive ecological index. The feature vector of the unified fusion shows that the PC1 weights for NDVI, WET, NDBSI, and LST are 0.612, 0.425, 0.525, and 0.413, respectively. Since the negative indicators NDBSI and LST have been reverse normalized, their eigenvectors are positive values.

Table 4. The result of principal component analysis.

Year	PC1		The eigenvector corresponding to each indicator			
	Eigenvalue	Eigen percent	NDVI	WET	NDBSI	LST
1990	0.134	75.3%	0.551	0.492	0.593	0.327
2000	0.141	75.8%	0.576	0.469	0.544	0.392
2010	0.186	81.0%	0.633	0.402	0.530	0.397
2020	0.194	85.3%	0.557	0.436	0.549	0.446
Convergence and unity	0.146	81.6%	0.612	0.425	0.525	0.413

Calculate the correlation coefficients between each indicator and the average correlation between URSEI and the individual indicators. The results are shown in Table 5, where all correlation coefficients pass the significance test at the 99% confidence level. The average correlation between URSEI and the ecological indicators for the four monitoring periods from 1990 to 2020 is 0.763, 0.733, 0.791, and 0.812, respectively, indicating that URSEI is a reasonable comprehensive ecological quality assessment metric. Furthermore, in all four monitoring periods, the average correlation of URSEI is higher than that of any single ecological indicator, demonstrating that URSEI is more suitable for evaluating ecological quality than individual indicators.

Table 5. Correlation matrix among URSEI and four indicators.

Year	Indicator	NDVI	WET	NDBSI	LST	URSEI
1990	NDVI	1	0.419	0.576	0.479	0.853
	WET	0.419	1	0.691	0.612	0.735
	NDBSI	0.576	0.691	1	0.652	0.769
	LST	0.479	0.612	0.652	1	0.693
	\bar{c}	0.491	0.574	0.640	0.581	0.763
2000	NDVI	1	0.492	0.608	0.591	0.720
	WET	0.492	1	0.647	0.654	0.648
	NDBSI	0.608	0.647	1	0.665	0.831
	LST	0.591	0.654	0.665	1	0.732
	\bar{c}	0.564	0.598	0.640	0.637	0.733
2010	NDVI	1	0.536	0.676	0.635	0.785
	WET	0.536	1	0.793	0.706	0.736

	NDBSI	0.676	0.793	1	0.729	0.858
	LST	0.635	0.706	0.729	1	0.783
	\bar{C}	0.616	0.678	0.733	0.690	0.791
	NDVI	1	0.587	0.831	0.605	0.822
	WET	0.587	1	0.788	0.753	0.787
2020	NDBSI	0.831	0.7788	1	0.765	0.864
	LST	0.605	0.753	0.765	1	0.774
	\bar{C}	0.674	0.706	0.795	0.708	0.812

3.2. Spatiotemporal Changes in Ecological Quality

To better quantify and visualize URSEI, this study follows literature [17] and classifies URSEI values into five levels at intervals of 0.2: [0–0.2), [0.2–0.4), [0.4–0.6), [0.6–0.8), and [0.8–1], representing poor, relatively poor, moderate, good, and excellent ecological quality, respectively. The classification maps of ecological quality in the GBA from 1990 to 2020 are shown in Figure 2.

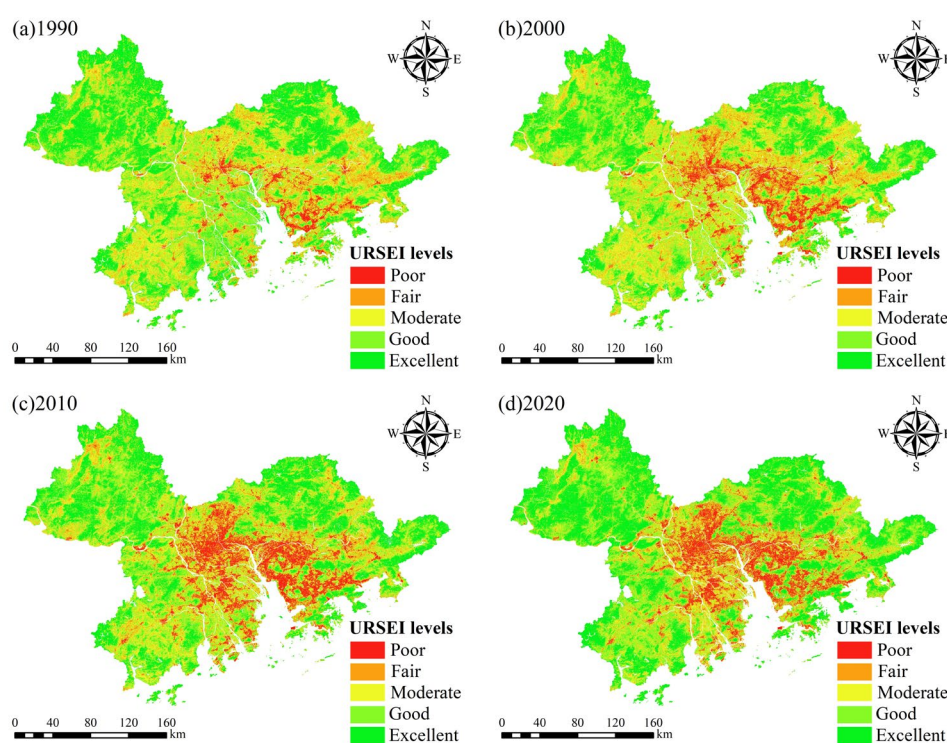


Figure 2. Spatial distribution of URSEI in the GBA from 1990 to 2020.

From 1990 to 2020, the spatial heterogeneity of ecological quality across the GBA was high, with significantly lower ecological quality in urban areas compared to non-urban areas. Over the 30-year period, ecological quality exhibited substantial changes with notable temporal variations. In 1990, areas classified as "poor" in ecological quality were relatively scattered, aligning with the geographic locations of built-up urban areas across the GBA, forming a distinct multi-center distribution pattern. Meanwhile, areas classified as "excellent" were mainly concentrated in the northeastern and northwestern parts of the GBA. By 2000, the extent of areas classified as "poor" had increased significantly compared to 1990, with major expansions occurring in Guangzhou, Dongguan, and Shenzhen along the eastern Pearl River estuary, as well as in Foshan, which is adjacent to Guangzhou. By 2010, the overall ecological quality of the GBA had further deteriorated, with a more pronounced spatial clustering of areas classified as "poor" in the central region. However, by 2020, the rate of ecological quality decline had slowed, with "poor" ecological quality areas remaining largely unchanged. At the same time, areas classified as "excellent" had significantly expanded in the northwestern and northeastern parts of the GBA.

Based on the URSEI classification results, the proportion of pixels in different ecological quality levels across the GBA from 1990 to 2020 was calculated, along with the mean URSEI values for the four monitoring periods. The results are shown in Figure 3. Over the past 30 years, the proportion of different URSEI levels has undergone varying degrees of change, with the overall mean URSEI showing a fluctuating downward trend. The mean URSEI values for the four years were 0.65, 0.60, 0.60, and 0.63, respectively, decreasing from 0.65 in 1990 to 0.63 in 2020. Compared to 1990, the ecological quality of the GBA in 2020 showed a slight decline. The proportions of areas classified as "excellent" and "good" remained relatively stable, while the proportion of "moderate" areas declined significantly. In contrast, the proportions of "poor" and "relatively poor" areas both increased, with the "poor" category rising notably from 2.54% in 1990 to 8.09% in 2020.

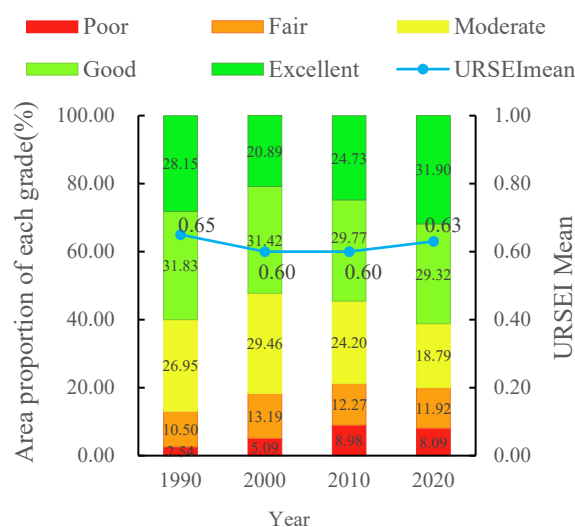


Figure 3. The proportion of area classified by ecological quality.

Based on the statistical analysis of the proportion of different ecological quality levels over each period, this study analyzed the ecological quality transitions in the GBA from 1990 to 2020 using transfer pathways (Figure 4). The results indicate that most ecological quality changes occurred between adjacent levels, exhibiting a gradual transition pattern where ecological quality progressively shifted from one level to the next. However, it is also important to note that some changes involved abrupt transitions across multiple levels, leading to significant ecological degradation. Examples include transitions from "moderate" to "poor," "good" to "poor," and "excellent" to "relatively poor." These areas require particular attention, and efforts should be intensified to strengthen ecological protection and environmental management. This is crucial to mitigating the immense pressure that economic and urbanization developments impose on the ecological environment.

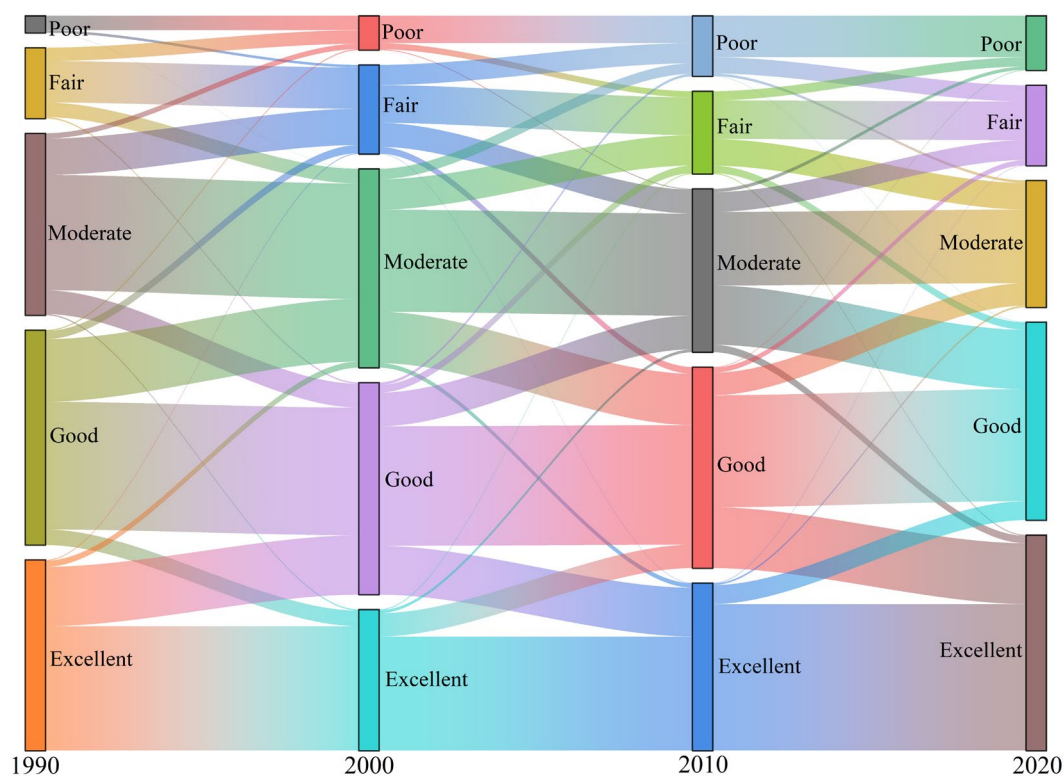


Figure 4. URSEI transfer matrix for the GBA,1990-2020.

3.3. Ecological Quality Change Detection

To further analyze the spatial and temporal distribution of ecological quality changes, this study applied a differencing method to detect variations in URSEI across multiple monitoring periods, using its five classification levels (Table 6).

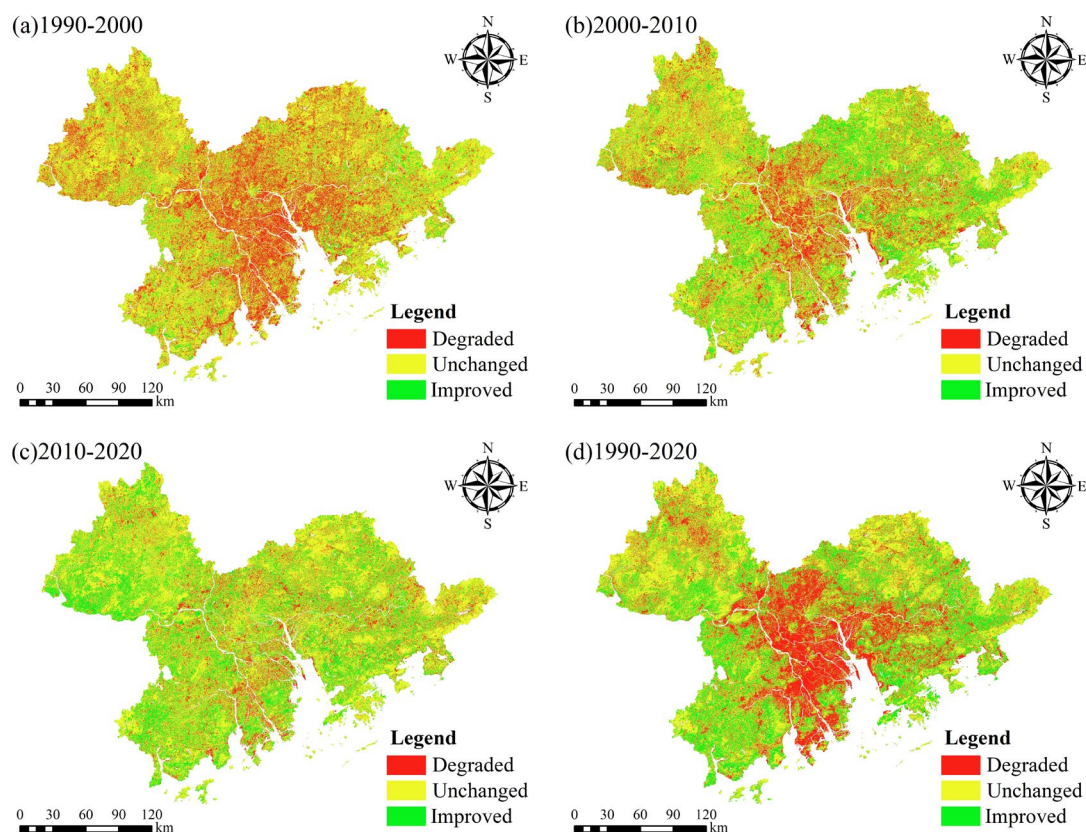
Table 7 and Figure 5 present the change detection results. From 1990 to 2000, the ecological quality of the GBA showed a declining trend, with a degradation area of 15,421.23 km², accounting for 28.61% of the total area. The spatial distribution of degradation was relatively uniform, affecting every city to varying degrees. Meanwhile, the proportion of improvement was only 8.78%, covering an area of 4,730.75 km². Between 2000 and 2010, ecological quality exhibited a more balanced trend, with the improvement area reaching 11,386.52 km² (21.13%) and the degradation area covering 10,533.77 km² (19.55%). The degradation zones were primarily concentrated in Guangzhou, Foshan, Dongguan, Shenzhen, and most parts of Zhongshan. From 2010 to 2020, ecological quality significantly improved, with an improvement area of 14,489.22 km², accounting for 26.89% of the total. The improvements were distributed across all cities, while the proportion of degraded areas dropped to 12.13%, mainly concentrated in the central region. Over the entire 30-year period (1990–2020), a total of 13,961.27 km² (25.95%) experienced ecological degradation. The most severe declines occurred in Guangzhou, Foshan, Zhongshan, Dongguan, and Zhuhai, while Zhaoqing, Huizhou, Jiangmen, and Shenzhen also exhibited varying degrees of degradation.

Table 6. Transfer matrix of ecological quality levels.

Level in end time	Level in start time				
	Poor	Fair	Moderate	Good	Excellent
Poor	Unchanged	Degraded	Degraded	Degraded	Degraded
Fair	Improved	Unchanged	Degraded	Degraded	Degraded
Moderate	Improved	Improved	Unchanged	Degraded	Degraded
Good	Improved	Improved	Improved	Unchanged	Degraded
Excellent	Improved	Improved	Improved	Improved	Unchanged

Table 7. Ecological quality level transfer matrix of in the GBA from 1990 to 2020.

Start and end time	Improved		Unchanged		Degraded	
	Area/km ²	Percentage/%	Area/km ²	Percentage/%	Area/km ²	Percentage/%
1990–2000	4730.75	8.78	33740.56	62.61	15421.23	28.61
2000–2010	11386.52	21.13	31972.04	59.33	10533.77	19.55
2010–2020	14489.22	26.89	32862.42	60.98	6537.97	12.13
1990–2020	13068.67	24.29	26773.19	49.76	13961.27	25.95

**Figure 5.** Change detection of ecological quality in the GBA from 1990 to 2020.

3.4. Ecological Quality Spatial Autocorrelation Analysis

To further explore the spatial aggregation characteristics of ecological quality in the GBA, this study adopts a $5 \text{ km} \times 5 \text{ km}$ grid to sample the URSEI values of each period, and uses GeoDa software to conduct spatial correlation analysis on the sampling results.

Global spatial autocorrelation shows (Table 8) that the Moran's I values of the GBA for all four periods are positive, and the significance test p-values are all less than 0.01, indicating that the ecological quality in the study area has a significant positive spatial autocorrelation feature, meaning regions with good or poor ecological quality tend to be spatially clustered. Among them, the Moran's I value for 2020 is the highest at 0.614, indicating the strongest spatial clustering of the ecological index in the GBA in 2020. Over the study period, the Moran's I value shows a gradual increasing trend over time."

Table 8. Global Moran's I value of ecological quality at different times in the GBA.

Year	Moran's I	z	p
1990	0.492	44.4	0.001
2000	0.565	50.99	0.001
2010	0.596	52.41	0.001
2020	0.614	54.43	0.001

In order to further investigate the specific locations where the ecological quality in the GBA shows spatial aggregation characteristics, local spatial autocorrelation analysis was conducted to generate LISA clustering maps, which were used to analyze the clustering phenomenon of the URSEI values in the study area. As shown in Figure 6, the high-high cluster areas show a clear high-value aggregation feature, and with the passage of time, the area of these clusters has increased. The high-high cluster areas are mainly distributed in the northwest in Zhaoqing City and in the northeast in Guangzhou and Huizhou Cities. These areas are mostly high-altitude regions, with contiguous forest development, high forest cover, minimal human socio-economic activities, low disturbance and damage to the ecological environment, and thus maintain a good ecological quality foundation with high protection levels, exhibiting well-preserved characteristics. The low-low cluster areas have also shown a clear increasing trend over the past 30 years, primarily located in central Guangzhou, Foshan, Dongguan, Shenzhen, and Zhongshan. In these areas, population density is high, urbanization levels are advanced, and land types are mainly built-up areas, where human activities intensively affect the ecological environment, leading to poor ecological quality. Overall, except for the insignificant regions, the high-high and low-low clustered areas of the four periods have relatively large and concentrated areas, while the high-low and low-high clustered areas are smaller and more dispersed in distribution.

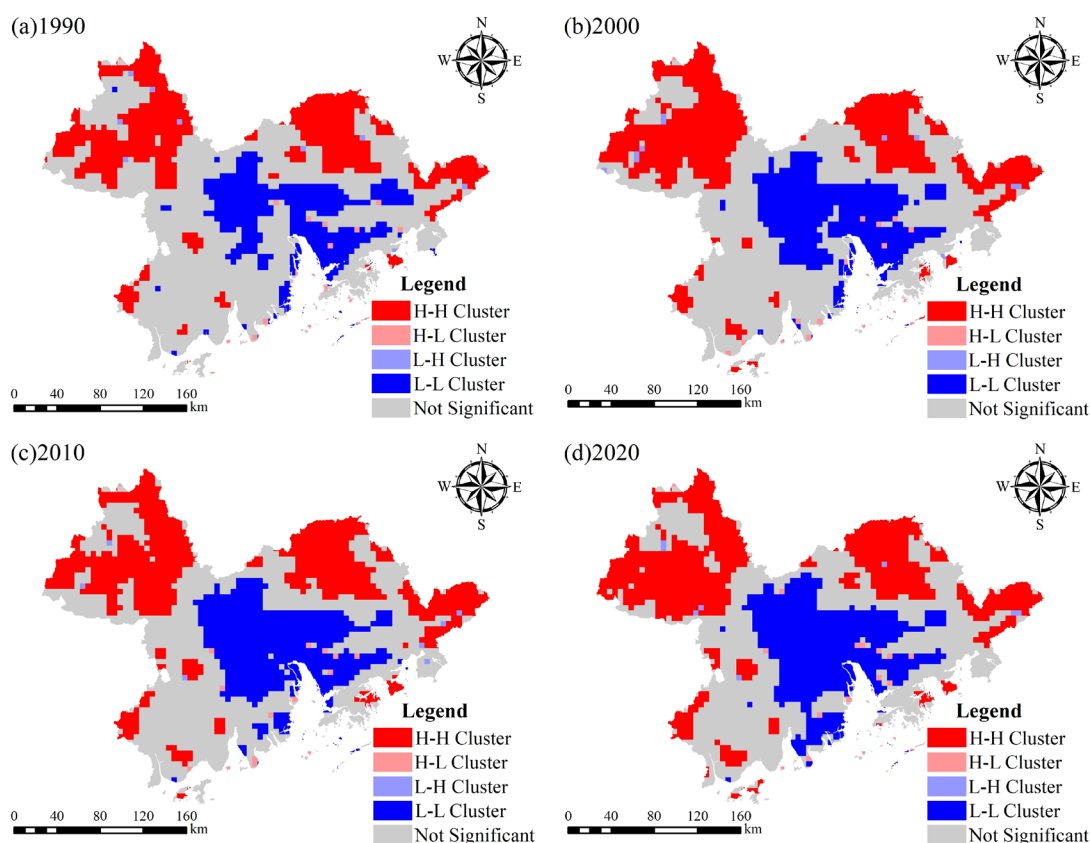


Figure 6. Locally autocorrelated LISA cluster map of ecological index in the GBA.

3.5. Ecological Quality Driving Factors Analysis

3.5.1. Single Factor Detection Results Analysis

The results of the single factor detection are shown in Table 9. The significance test p-values of all factors are less than 0.001, indicating that the selected independent variables significantly impact the spatial differentiation of ecological quality in the GBA.

From the average q-values of the factors for the four monitoring years, nighttime lighting, GDP, and temperature exhibit a strong explanatory power for the spatial differentiation of ecological quality, with average q-values of 0.334, 0.305, and 0.302, respectively, all exceeding 0.3. This suggests

that these factors play a dominant role in the spatial differentiation of ecological quality. The next most important factors are elevation, land use type, population density, and slope, with average q-values ranging from 0.2 to 0.3, indicating a moderate explanatory power for URSEI spatial differentiation. Precipitation has the weakest influence, with an average q-value of only 0.042.

From a temporal perspective, the q-values of the factors fluctuate dynamically, and the relative importance of some factors has significantly changed. In 1990, land use type had a relatively weak explanatory power for ecological spatial heterogeneity, with a q-value of 0.145, ranking seventh. However, by 2020, the q-value increased to 0.328, rising to third place. In 1990, temperature was the dominant factor influencing ecological quality spatial differentiation, while in 2000, 2010, and 2020, the nighttime lighting index became the primary influencing factor, indicating that the dominant factors of ecological quality spatial differentiation in the Greater Bay Area shifted from natural to human factors.

Overall, the spatial differentiation of ecological quality in the GBA is influenced by both natural and human factors. In the early stages of the study period, natural factors had a stronger influence on ecological quality spatial differentiation, while in the later stages, human factors had a greater impact than natural factors, reflecting the profound impact of the rapid urbanization process in the GBA on the ecological environment."

Table 9. The result of single detection from 1990 to 2020.

Factor	1990		2000		2010		2020		2000-2020	
	q value	sort	q value	sort						
Temperature	0.288	1	0.296	2	0.320	3	0.305	4	0.302	3
Precipitation	0.037	8	0.065	8	0.037	8	0.028	8	0.042	8
DEM	0.243	2	0.271	4	0.267	5	0.268	5	0.262	4
Slope	0.181	5	0.208	7	0.232	7	0.256	6	0.219	7
Type of land use	0.145	7	0.218	6	0.282	4	0.328	3	0.243	5
Population density	0.158	6	0.238	5	0.235	6	0.213	7	0.211	6
GDP	0.208	4	0.294	3	0.350	2	0.369	2	0.305	2
Nighttime lights	0.235	3	0.338	1	0.353	1	0.409	1	0.334	1

3.5.2. Interaction Detection Results Analysis

An interaction detection analysis was conducted on the influencing factors, and the results are shown in Figure 7. Except for the interaction between precipitation and temperature in 1990 and the nonlinear enhancement effects of precipitation interacting with elevation, land use type, and population density in 2020, all other factor interactions exhibited a bivariate enhancement effect. This indicates that the spatial differentiation of ecological quality in the GBA is not the direct, independent result of a single factor but is instead driven by the synergistic enhancement effect of factor interactions.

From 1990 to 2020, the highest-ranked interactions in terms of q-value were as follows: temperature \cap GDP (0.370) in 1990, nighttime light index \cap elevation (0.422) in 2000, temperature \cap GDP (0.451) in 2010, and nighttime light \cap land use type (0.495) in 2020. Over the 30-year period, the interaction q-value steadily increased from 0.370 to 0.495. Before 2010, interactions between natural and human factors had a more pronounced impact on ecological quality. However, in 2020, interactions among human factors had the greatest influence, reflecting the increasing role of socio-economic development and human activities in ecological quality changes.

By combining these findings with the single-factor detection results, it becomes evident that although precipitation had weak explanatory power when acting alone, its q-value increased significantly when interacting with other factors. This suggests that under the influence of factor interactions, single factors with initially low explanatory power can be significantly enhanced through synergistic effects, improving their ability to explain spatial differentiation in ecological quality.

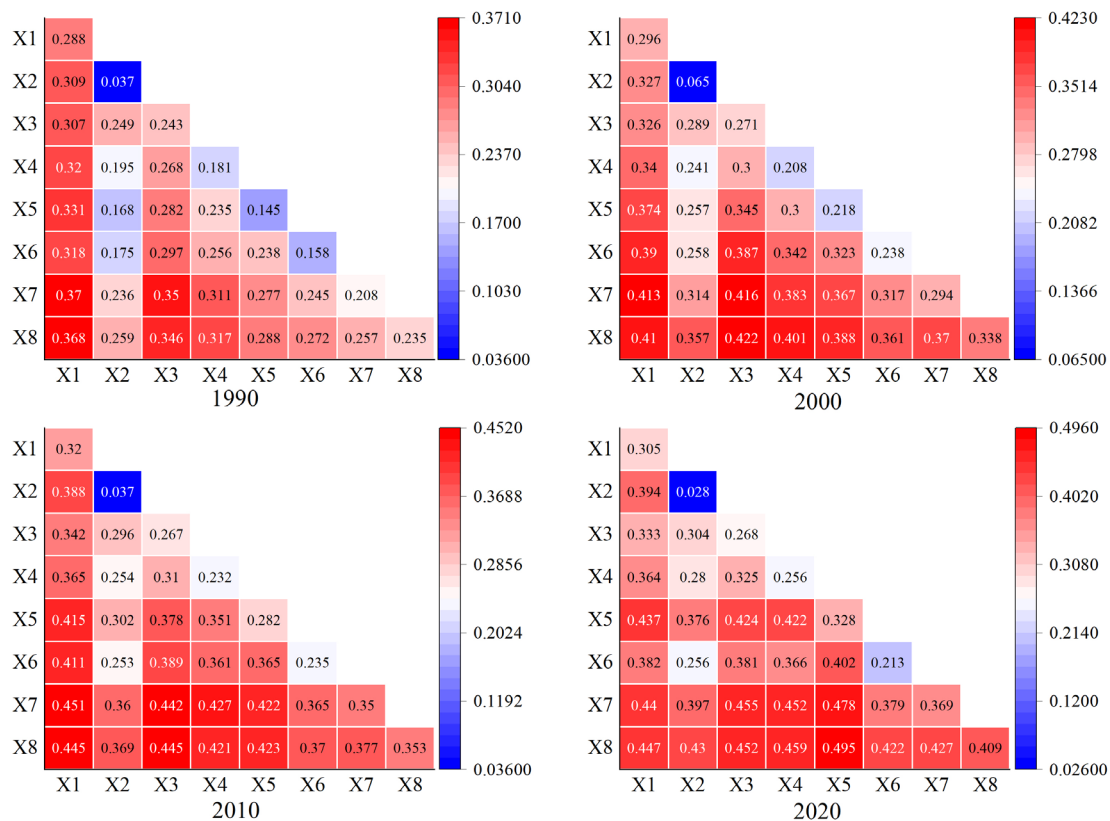


Figure 7. Interactive detection result of driving factors of ecological quality. Note: X1: (Temperature), X2: (Precipitation), X3: (DEM), X4: (Slope), X5: (Type of land use), X6: (Population density), X7: (GDP), X8: (Nighttime lights).

3.5.3. Risk Zone Detection Analysis

Risk zone detection is used to determine whether there are significant differences in the mean attribute values of different partitions of each factor. In this study, the risk zone detection method was applied to identify the optimal range for quantitative factors and the most suitable type for qualitative factors affecting URSEI. The 2020 risk detection results were selected as an example for analysis.

As shown in Table 10, the 2020 risk detection results indicate a significant negative correlation between the intensity of human factors and the URSEI mean value. Specifically, the three human-related factors—population density, GDP, and nighttime light index—were classified into five levels, with Level 1 representing the lowest value range and Level 5 representing the highest. The analysis results show that for all three factors, the highest URSEI mean values appeared in Level 1, with values of 0.698 (population density), 0.739 (GDP), and 0.8 (nighttime light index). Their optimal ranges were further determined to be 73–1466 people/km², 0.04–12.05 million yuan/km², and 0–19, respectively. These findings suggest that human activities have a significant impact on the ecological quality of the Guangdong-Hong Kong-Macau Greater Bay Area, with lower human activity intensity corresponding to higher URSEI values, indicating better ecological quality. Additionally, when the land use type was forest, the URSEI mean value was the highest, highlighting the crucial role of forest ecosystems in maintaining high ecological quality.

Among natural factors, temperature also exhibited a negative correlation with URSEI, with the highest URSEI mean value occurring at Temperature Level 1 (15.52–19.74°C), suggesting that areas with lower temperatures tend to have better ecological quality. In terms of elevation and slope classifications, the highest URSEI mean values appeared in Level 4 and Level 5, respectively, indicating that regions with high elevations and steep slopes tend to have better ecological quality, possibly due to lower human disturbance. The precipitation classification results show that the highest URSEI mean value (0.703) was found in Level 5, corresponding to a precipitation range of

1930–2116 mm, suggesting that higher precipitation levels may contribute to maintaining ecological conditions.

Table 10. The appropriate type and range of factors.

Factor	Suitability	The scope or category corresponding to the level of adaptation	RSEI mean
Temperature	1	15.52~19.74 °C	0.865
Precipitation	5	1930~2116 mm	0.703
DEM	4	393~651 m	0.863
Slope	5	8.52~18.77°	0.841
Type of land use	4	woodland	0.739
Population density	1	73~1466 people·km ⁻²	0.698
GDP	1	0.04~12.05 million yuan·km ⁻²	0.739
Nighttime lights	1	0~19	0.800

4. Discussion

4.1. Applicability Analysis of the URSEI Model

The RSEI has been widely used due to its easy data acquisition, simple calculation, and the absence of manually assigned weights and thresholds. However, when applying RSEI for long-term ecological quality assessments, the consistency and comparability of time-series evaluation results are often affected by factors such as data acquisition time and weather variations. Additionally, the multiple normalization processes in the RSEI model make the assessment results more dependent on the relative ecological conditions within the study area. In regions with drastic ecological changes, such as the Guangdong-Hong Kong-Macau Greater Bay Area, this dependence further weakens the consistency and comparability of time-series analysis results.

The method proposed in this study introduces several improvements, including optimized data selection, refined index synthesis, normalization of invariant region indicators, and multi-temporal principal component fusion analysis, leading to the development of the URSEI. These enhancements effectively overcome the limitations of RSEI in monitoring long-term ecological dynamics in cloud-prone and ecologically volatile regions. URSEI enables spatial visualization and pattern analysis of ecological quality changes in the Greater Bay Area over different time periods, demonstrating two major improvements:

First, in the URSEI classification maps for 1990–2020 (Figure 2), there are no apparent edge-matching or mosaic traces, and the spatial distribution of ecological quality remains highly consistent across different time periods. This ensures the coherence and integrity of the study results, enhancing the visualization of ecological quality distribution. Second, in the ecological quality change detection maps from 1990 to 2020 (Figure 5), no significant anomalies are observed, and the identified ecological change areas align well with real-world conditions. This indicates that the URSEI model effectively maintains comparability in long-term time-series analysis.

Under the challenging conditions of high cloud cover, frequent rainfall, and rapid ecological changes in the GBA, the URSEI model demonstrates strong applicability and reliability. Its improved normalization method and multi-temporal principal component fusion analysis technique not only enhance the consistency and comparability of ecological quality assessments but also provide robust support for accurately analyzing long-term ecological evolution trends. In the future, the URSEI model can be further extended to other regions with similar climatic conditions and ecological variations, offering scientific support for regional ecological protection and sustainable development.

4.2. Spatiotemporal Evolution Characteristics and Influencing Factors of Ecological Quality in the GBA

Based on the spatiotemporal variation analysis of the URSEI, this study reveals the significant characteristics and driving mechanisms of ecological quality evolution in the GBA over the past 30

years (1990–2020). The results indicate that ecological quality changes in the GBA exhibit distinct phased characteristics, with 2010 serving as a turning point, dividing the evolution into two stages.

In the first stage (1990–2010), the GBA experienced a significant decline in ecological quality. This trend is closely associated with rapid industrialization and urbanization in the region. During this period, cities on the eastern shore of the Pearl River Estuary, such as Guangzhou, Shenzhen, and Dongguan, served as the frontiers of China's economic reform, where industrial expansion and urban development progressed simultaneously, leading to a substantial increase in human activity intensity. Unregulated land use practices and declining vegetation cover contributed to severe environmental degradation. Between 2000 and 2010, as industrial relocation and upgrading occurred, low-end manufacturing industries gradually shifted to western cities such as Foshan, Jiangmen, and Zhongshan, further exacerbating regional ecological deterioration.

In the second stage (2010–2020), ecological quality in the GBA showed an improving trend. This shift can be attributed to several key factors. First, the pace of urbanization slowed down, and the expansion of industrial land significantly decreased. Second, a series of ecological protection policies and regulations were successively introduced at both provincial and municipal levels, strengthening ecosystem conservation, monitoring, and restoration efforts. Lastly, the regional industrial structure gradually transitioned toward high-tech industries, effectively reducing the ecological pressure from traditional industrial sectors. Notably, Zhaoqing and Huizhou, serving as ecological barriers in the northern and eastern parts of the GBA, maintained relatively stable ecological quality throughout the study period, highlighting their crucial ecological protection functions.

From a spatial perspective, the ecological quality of the GBA exhibits significant spatial heterogeneity. The central urban cluster, including Guangzhou, Foshan, Dongguan, Shenzhen, and Zhongshan, generally shows lower ecological quality due to intensive human activities. In contrast, the northwestern and northeastern regions, such as Zhaoqing and Huizhou, benefit from favorable topographic conditions, high vegetation coverage, and lower human disturbances, maintaining relatively high ecological quality levels. This spatial differentiation pattern is strongly coupled with regional economic development levels and human activity intensity.

Geographical detector analysis results indicate that the spatial differentiation of ecological quality in the GBA is driven by both natural and anthropogenic factors. Among these, nighttime light intensity, GDP, and temperature are the primary drivers of ecological quality variations. From a temporal perspective, human activity-related factors, such as land use type, population density, GDP, and nighttime light index, have shown an increasing explanatory power for URSEI over time, while the influence of natural factors has remained relatively stable. This finding confirms the dominant role of human activities in shaping ecological quality changes in the GBA, reflecting the profound impact of rapid urbanization on the region's ecological landscape.

4.3. Ecological Protection and Sustainable Development Recommendations for the GBA

Based on the assessment results of the URSEI, the ecological quality of the GBA has undergone significant spatiotemporal changes over the past 30 years. Particularly during the rapid urbanization and industrialization processes, some areas have experienced noticeable ecological degradation. To address these challenges and ensure the sustainable development of the regional ecosystem, this study proposes the following ecological protection and sustainability recommendations tailored to the GBA's regional characteristics:

(1) The northwestern and northeastern parts of the GBA (e.g., Zhaoqing and Huizhou) exhibit high ecological quality and a distinct high-high clustering pattern. These areas are predominantly high-altitude regions with dense forest coverage and minimal human disturbance, serving as crucial ecological barriers for the region. It is recommended to strengthen ecological redline management, strictly control the expansion of construction land to prevent ecological degradation, and enhance the protection of nature reserves and ecological function zones to improve the stability and resilience of regional ecosystems.

(2) The central urban cluster (e.g., Guangzhou, Shenzhen, Foshan, Dongguan, and Zhongshan) exhibits relatively low ecological quality due to intensive human activities. It is recommended that these cities optimize land use structure, curb the disorderly expansion of construction land, and increase green spaces and water bodies to enhance the stability and resilience of urban ecosystems. Specific measures include promoting urban greening projects by expanding parks and green areas, strengthening water body protection by restoring and rehabilitating wetland ecosystems, and advocating for green buildings and low-carbon city development to mitigate the urban heat island effect.

(3) In industrially intensive areas such as Foshan and Dongguan, ecological degradation is particularly evident. It is recommended to continue promoting industrial upgrading, phasing out outdated production capacities, reducing industrial pollution, and improving ecological environmental quality. Specific measures include encouraging enterprises to adopt clean production technologies to minimize pollutant emissions, strengthening environmental supervision of industrial parks to ensure compliance with emission standards, and promoting green manufacturing and a circular economy to enhance resource efficiency.

(4) The GBA encompasses multiple cities and administrative regions, making cross-regional cooperation and coordination essential for improving ecological quality. It is recommended that cities strengthen collaborative governance in ecological protection, jointly addressing environmental challenges to ensure the integrity and sustainability of the regional ecosystem. Specific measures include establishing a cross-regional ecological protection coordination mechanism, formulating unified ecological protection policies and standards, enhancing the sharing and monitoring of ecological data to improve the scientific precision of regional environmental management, and promoting an ecological compensation mechanism to balance environmental protection with economic development.

5. Conclusions

This study introduces the URSEI as an enhancement of the traditional RSEI. Through optimization of data selection, normalization of invariant region indicators, and multi-temporal principal component analysis, URSEI effectively addresses the challenges of ecological quality assessment in the cloud and rainy climate of the GBA. The dynamic monitoring results from 1990 to 2020 show significant improvements in the consistency and spatial visualization of ecological assessments.

The findings reveal that the ecological quality of the GBA exhibits a spatial distribution characterized by lower values in the central region and higher values in the northwest and northeast areas. The URSEI values over the years show a trend of decline followed by improvement, with an overall slight degradation of ecological quality, as evidenced by a 24.29% improvement area and a 25.95% degradation area. The spatial analysis indicates a significant positive spatial autocorrelation, with high-high and low-low clustering patterns dominating, which align with the changes in URSEI grades.

The spatial differentiation of ecological quality is influenced by both natural and anthropogenic factors. Key drivers of spatial variation include nighttime light intensity, GDP, and temperature, with human factors having a stronger impact, which has increased over time. This study underscores the importance of considering both natural and human influences in long-term ecological monitoring and provides a reliable method for assessing ecological quality in regions with varying climatic and environmental conditions.

Author Contributions: Conceptualization, F.S. and C.D.; methodology, H.L. and L.Z.; software, L.W.; validation, F.S., C.D. and H.L.; formal analysis, R.J. and L.Z.; investigation, R.J. and H.L.; resources, J.C. and F.S.; data curation, R.J. and H.L.; writing—original draft preparation, R.J. and H.L.; writing—review and editing, F.S. and C.D.; visualization, R.J. and L.Z.; supervision, L.W. and J.C.; project administration, J.C.; funding acquisition, F.S. and H.L. All authors have read and agreed to the published version of the manuscript.

Funding: This research was funded by the Scientific research project of Ecology Environment Bureau of Shenzhen Municipality, grant number SZDL2023001387, the Fundamental Research Foundation of Shenzhen Technology and Innovation Council, grant number JCYJ20220818101617038, the National Natural Science Foundation of China, grant number 42271353, and the Guangdong Basic and Applied Basic Research Foundation, grant number 2024A1515011858.

Institutional Review Board Statement: Not applicable

Informed Consent Statement: Not applicable.

Data Availability Statement: The data presented in this study are available within the article.

Conflicts of Interest: The authors declare no conflict of interest.

References

1. Zeng, S.Y.; Ma, J.; Yang, Y.J.; Zhang, S.L.; Liu, G.J.; Chen, F. Spatial assessment of farmland soil pollution and its potential human health risks in China. *Sci. Total Environ.* **2019**, *687*, 642-653.
2. Mahmoud, S.H.; Gan, T.Y. Impact of anthropogenic climate change and human activities on environment and ecosystem services in arid regions. *Sci. Total Environ.* **2018**, *633*, 1329-1344.
3. Wang, X.; Lu, B.B.; Li, J.S.; Liu, Q.Y.; He, L.H.; Lv, S.C.; Yu, S.H. Spatio-temporal analysis of ecological service value driven by land use changes: A case study with Danjiangkou, Hubei section. *Resour. Environ. Sustain.* **2024**, *15*.
4. Fang, C.L.; Wang, Z.B.; Liu, H.M. Exploration on the theoretical basis and evaluation plan of Beautiful China construction. *Acta Geogr. Sin.* **2019**, *74*, 619-632.
5. Yu, G.R.; Wang, Y.S.; Yang, M. Discussion on the ecological theory and assessment methods of ecosystem quality and its evolution. *Chin. J. Appl. Ecol.* **2022**, *33*, 865-877.
6. Li, J.Q.; Tian, Y. Assessment of Ecological Quality and Analysis of Influencing Factors in Coal-Bearing Hilly Areas of Northern China: An Exploration of Human Mining and Natural Topography. *Land* **2024**, *13*.
7. Xu, T.; Wu, H. Spatiotemporal Analysis of Vegetation Cover in Relation to Its Driving Forces in Qinghai-Tibet Plateau. *Forests* **2023**, *14*.
8. Wang, R.; Ding, X.; Yi, B.J.; Wang, J.L. Spatiotemporal characteristics of vegetation cover change in the Central Yunnan urban agglomeration from 2000 to 2020 based on Landsat data and its driving factors. *Geocarto Int.* **2024**, *39*.
9. Wang, Y.L.; Zhang, A.; Gao, X.T.; Zhang, W.; Wang, X.H.; Jiao, L.L. Spatial-Temporal Differentiation and Driving Factors of Vegetation Landscape Pattern in Beijing-Tianjin-Hebei Region Based on the ESTARFM Model. *Sustainability* **2024**, *16*.
10. Yuan, D.B.; Zhang, L.Y.; Fan, Y.Q.; Sun, W.B.; Fan, D.Q.; Zhao, X.R. Spatio-Temporal Analysis of Surface Urban Heat Island and Canopy Layer Heat Island in Beijing. *Appl. Sci.-Basel* **2024**, *14*.
11. Chen, X.; Zhang, S.C.; Tian, Z.Y.; Luo, Y.Q.; Deng, J.; Fan, J.H. Differences in urban heat island and its driving factors between central and new urban areas of Wuhan, China. *Environ. Sci. Pollut. Res.* **2023**, *30*, 58362-58377.
12. Miao, S.; Liu, C.; Qian, B.J.; Miao, Q. Remote sensing-based water quality assessment for urban rivers: a study in linyi development area. *Environ. Sci. Pollut. Res.* **2020**, *27*, 34586-34595.
13. Zheng, Z.H.; Wu, Z.F.; Chen, Y.B.; Yang, Z.W.; Marinello, F. Exploration of eco-environment and urbanization changes in coastal zones: A case study in China over the past 20 years. *Ecol. Indic.* **2020**, *119*.
14. Li, C.; Chen, T.; Jia, K.; Plaza, A. Coupling Analysis Between Ecological Environment Change and Urbanization Process in the Middle Reaches of Yangtze River Urban Agglomeration, China. *IEEE J. Sel. Top. Appl. Earth Observ. Remote Sens.* **2024**, *17*, 880-892.

15. Wang, C.; Sheng, Q.; Zhu, Z. Exploring Ecological Quality and Its Driving Factors in Diqing Prefecture, China, Based on Annual Remote Sensing Ecological Index and Multi-Source Data. *Land* **2024**, *13*, 1499-1499.
16. Xu, H.; Wang, Y.; Guan, H.; Shi, T.; Hu, X. Detecting Ecological Changes with a Remote Sensing Based Ecological Index (RSEI) Produced Time Series and Change Vector Analysis. *Remote Sens.* **2019**, *11*, 2345-2345.
17. Xu, H.Q. A remote sensing index for assessment of regional ecological changes. *China Environ. Sci.* **2013**, *33*, 889-897.
18. Gan, X.T.; Du, X.C.; Duan, C.J.; Peng, L.H. Evaluation of Ecological Environment Quality and Analysis of Influencing Factors in Wuhan City Based on RSEI. *Sustainability* **2024**, *16*.
19. Chen, Z.Y.; Chen, R.R.; Guo, Q.; Hu, Y.L. Spatiotemporal Change of Urban Ecologic Environment Quality Based on RSEI-Taking Meizhou City, China as an Example. *Sustainability* **2022**, *14*.
20. Zhang, L.; Hou, Q.; Duan, Y.; Ma, S. Spatial and Temporal Heterogeneity of Eco-Environmental Quality in Yanhe Watershed (China) Using the Remote-Sensing-Based Ecological Index (RSEI). *Land* **2024**, *13*, 780-.
21. He, Y.R.; Chen, Y.H.; Zhong, L.; Lai, Y.F.; Kang, Y.T.; Luo, M.; Zhu, Y.F.; Zhang, M. Spatiotemporal evolution of ecological environment quality and its drivers in the Helan Mountain, China. *J. Arid Land* **2025**, *17*, 224-244.
22. Cai, C.; Li, J.Y.; Wang, Z.Q. Long-Term Ecological and Environmental Quality Assessment Using an Improved Remote-Sensing Ecological Index (IRSEI): A Case Study of Hangzhou City, China. *Land* **2024**, *13*.
23. Feng, Z.X.; She, L.; Wang, X.H.; Yang, L.; Yang, C. Spatial and Temporal Variations of Ecological Environment Quality in Ningxia Based on Improved Remote Sensing Ecological Index. *Ecol. Environ. Sci.* **2024**, *33*, 131-143.
24. Cheng, L.L.; Wang, Z.W.; Tian, S.F.; Liu, Y.T.; Sun, M.Y.; Yang, Y.M. Evaluation of eco-environmental quality in Mentougou District of Beijing based on improved remote sensing ecological index. *Chin. J. Ecol.* **2021**, *40*, 1177-1185.
25. Ke, L.N.; Xu, J.H.; Wang, N.; Hou, J.X.; Han, X.; Yin, S.S. Evaluation of Ecological Quality of Coastal Wetland Based on Remote Sensing Ecological Index: A Case Study of Northern Liaodong Bay. *Ecol. Environ. Sci.* **2022**, *31*, 1417-1424.
26. Liu, Y.; Dang, C.Y.; Yue, H.; Lu, C.G.; Qian, J.X.; Zhu, R. Comparison between modified remote sensing ecological index and RSEI. *J. Remote Sens.* **2022**, *26*, 683-697.
27. Jianwei, G.; Kunyong, Y.; Zhen, X.; Gejin, Z.; Jingwen, A.; Liuqing, Y.; Honghui, Y.; Jian, L. Analysis of Spatiotemporal Variation and Drivers of Ecological Quality in Fuzhou Based on RSEI. *Remote Sens.* **2022**, *14*, 4900-4900.
28. Chen, N.; Cheng, G.; Yang, J.; Ding, H.; He, S. Evaluation of Urban Ecological Environment Quality Based on Improved RSEI and Driving Factors Analysis. *Sustainability* **2023**, *15*.
29. Liu, Y.; Zhou, T.; Yu, W. Analysis of Changes in Ecological Environment Quality and Influencing Factors in Chongqing Based on a Remote-Sensing Ecological Index Mode. *Land* **2024**, *13*.
30. Long, T.; Bai, Z.; Zheng, B. Spatiotemporal Dynamics and Driving Forces of Ecological Environment Quality in Coastal Cities: A Remote Sensing and Land Use Perspective in Changle District, Fuzhou. *Land* **2024**, *13*, 1393-1393.
31. Yue, H.; Liu, Y.; Li, Y.; Lu, Y. Eco-Environmental Quality Assessment in China's 35 Major Cities Based On Remote Sensing Ecological Index. *IEEE Access* **2019**, *7*, 51295-51311.
32. He, Y. Construction of qualitative assessment model of ecological environment quality under river safety remediation. *Int. J. Environ. Technol. Manag.* **2024**, *27*.

33. Wang, J.Y.; Chen, G.; Yuan, Y.R.; Fei, Y.; Xiong, J.N.; Yang, J.W.; Yang, Y.M.; Li, H. Spatiotemporal changes of ecological environment quality and climate drivers in Zoige Plateau. *Environ. Monit. Assess.* **2023**, *195*.
34. Liu, W.M.; Cheng, Z.Y.; Li, J.; Li, G.; Pan, N.H. Assessment of ecological asset quality and its drivers in Agro-pastoral Ecotone of China. *Ecol. Indic.* **2025**, *170*.
35. Zeng, J.W.; Dai, X.; Li, W.Y.; Xu, J.P.; Li, W.L.; Liu, D.S. Quantifying the Impact and Importance of Natural, Economic, and Mining Activities on Environmental Quality Using the PIE-Engine Cloud Platform: A Case Study of Seven Typical Mining Cities in China. *Sustainability* **2024**, *16*.
36. Zhitao, L.; Shaojian, W.; Chuanglin, F. Spatiotemporal evolution and influencing mechanism of ecosystem service value in the Guangdong-Hong Kong-Macao Greater Bay Area. *J. Geogr. Sci.* **2023**, *33*, 1226-1244.
37. Ren, Y.F.; He, X.N.; Jiang, Q.N.; Zhang, F.; Zhang, B.T. Advancing high-quality development in China: Unraveling the dynamics, disparities, and determinants of inclusive green growth at the prefecture level. *Ecol. Indic.* **2024**, *169*.
38. Pharaoh, E.; Diamond, M.; Jarvie, H.P.; Ormerod, S.J.; Rutt, G.; Vaughan, I.P. Potential drivers of changing ecological conditions in English and Welsh rivers since 1990. *Sci. Total Environ.* **2024**, *946*.
39. Wang, J.F.; Xu, C.D. Geodetector: Principle and prospective. *Acta Geogr. Sin.* **2017**, *72*, 116-134.
40. Ju, H.; Zhang, Z.; Zuo, L.; Wang, J.; Zhang, S.; Wang, X.; Zhao, X. Driving forces and their interactions of built-up land expansion based on the geographical detector – a case study of Beijing, China. *Int. J. Geogr. Inf. Sci.* **2016**, *30*, 2188-2207.
41. Tao, S.; Yi, C.; Weidong, L.; Hui, L. Spatial difference and mechanisms of influence of geo-economy in the border areas of China. *J. Geogr. Sci.* **2017**, *27*, 1463-1480.
42. Zuo, S.; Dai, S.; Song, X.; Xu, C.; Liao, Y.; Chang, W.; Chen, Q.; Li, Y.; Tang, J.; Man, W.; et al. Determining the Mechanisms that Influence the Surface Temperature of Urban Forest Canopies by Combining Remote Sensing Methods, Ground Observations, and Spatial Statistical Models. *Remote Sens.* **2018**, *10*, 1814-1814.
43. Liang, P.; Yang, X. Landscape spatial patterns in the Maowusu (Mu Us) Sandy Land, northern China and their impact factors. *Catena* **2016**, *145*, 321-333.
44. Huang, J.; Wang, J.; Bo, Y.; Xu, C.; Hu, M.; Huang, D. Identification of Health Risks of Hand, Foot and Mouth Disease in China Using the Geographical Detector Technique. *Int. J. Environ. Res. Public Health* **2014**, *11*, 3407-3423.
45. Zhang, H.J. Ecological environment change in Guangdong-Hong Kong-Macao Greater Bay Area based on multi-temporal remote sensing ecological index. *Sci. Geogr. Sin.* **2019**, *8*, 8.
46. Yang, C.; Zhang, C.; Li, Q.; Liu, H.; Gao, W.; Shi, T.; Liu, X.; Wu, G. Rapid urbanization and policy variation greatly drive ecological quality evolution in Guangdong-Hong Kong-Macao Greater Bay Area of China: A remote sensing perspective. *Ecol. Indic.* **2020**, *115*.
47. Wu, Y.Y.; Luo, Z.H.; Wu, Z.F. Exploring the Relationship between Urbanization and Vegetation Ecological Quality Changes in the Guangdong-Hong Kong-Macao Greater Bay Area. *Land* **2024**, *13*.
48. Wang, Y.; Zhao, Y.H.; Wu, J.S. Dynamic monitoring of long time series of ecological quality in urban agglomerations using Google Earth Engine cloud computing: A case study of the Guangdong-Hong Kong-Macao Greater Bay Area, China. *Acta Ecol. Sin.* **2020**, *40*, 8461-8473.
49. Wu, B.F. *ChinaCover*; Science Press: Beijing, 2017; p. 397.
50. Liu, J.C.; Xie, T.; Lyu, D.; Cui, L.; Liu, Q.M. Analyzing the Spatiotemporal Dynamics and Driving Forces of Ecological Environment Quality in the Qinling Mountains, China. *Sustainability* **2024**, *16*.
51. Ding, X.; Shao, X.; Wang, J.L.; Peng, S.Y.; Shi, J.C. Research on the Spatial-Temporal Pattern Evolution and Driving Force of Ecological Environment Quality in Kunming City Based on Remote Sensing Ecological Environment Index in the Past 25 Years. *Pol. J. Environ. Stud.* **2024**, *33*, 1073-1089.

52. Wang, X.Y.; Wang, X.D.; Jin, X.; Kou, L.D.; Hou, Y.J. Evaluation and driving force analysis of ecological environment in low mountain and hilly regions based on optimized ecological index. *Sci Rep* **2024**, *14*.
53. Zhang, S.W.; Wang, Y.; Wang, X.H.; Wu, Y.; Li, C.R.; Zhang, C.; Yin, Y.H. Ecological Quality Evolution and Its Driving Factors in Yunnan Karst Rocky Desertification Areas. *Int. J. Environ. Res. Public Health* **2022**, *19*.
54. Zhu, Z.R.; Cao, H.S.; Yang, J.C.; Shang, H.; Ma, J.Q. Ecological environment quality assessment and spatial autocorrelation of northern Shaanxi mining area in China based-on improved remote sensing ecological index. *Front. Environ. Sci.* **2024**, *12*.
55. Wang, S.D.; Si, J.J.; Wang, Y. Study on Evaluation of Ecological Environment Quality and Temporal-Spatial Evolution of Danjiang River Basin (Henan Section). *Pol. J. Environ. Stud.* **2021**, *30*, 2353-2367.
56. Jiao, K.; Yong, X.Q.; Mao, S.H.; Chen, K.Y. Analysis of the evolution and influencing factors of ecological environment quality after the transformation of resource-exhausted cities based on GEE and RSEI: a case study of Xuzhou City, China. *J. Asian Archit. Build. Eng.* **2024**.
57. QianQian, X.; YaNing, C.; XueQi, Z.; JianLi, D. Spatiotemporal Changes in Ecological Quality and Its Associated Driving Factors in Central Asia. *Remote Sens.* **2022**, *14*, 3500-3500.

Disclaimer/Publisher's Note: The statements, opinions and data contained in all publications are solely those of the individual author(s) and contributor(s) and not of MDPI and/or the editor(s). MDPI and/or the editor(s) disclaim responsibility for any injury to people or property resulting from any ideas, methods, instructions or products referred to in the content.